CHEMICAL ENGINEERING TRANSACTIONS
VOL. 70, 2018
A publication of AIDIC
The Italian Association of Chemical Engineering
Online at www.aidic.it/cet
Guest Editors: Timothy G. Walmsley, Petar S. Varbanov, Rongxin Su, Jiří J. Klemeš

ISBN 978-88-95608-67-9; **ISSN** 2283-9216
DOI: 10.3303/CET1870090

Exergy Recovery During Liquefied Natural Gas Regasification Using Methane as Working Fluid

Francesca Belfiore*, Francesco Baldi, François Maréchal

École Polytechnique Fédérale de Lausanne (EPFL Valis Wallis), SCI-STI-FM, Industrial Process and Energy Systems Engineering (IPESE), Rue de l'Industrie 17, Case postale 440, CH-1951 Sion, Switzerland
francesca.belfiore@epfl.ch

The increased concerns about the effect of human activities on the climate have pushed natural gas among the most obvious solutions for the transition to a low-carbon economy. The growing importance and volumes of liquefied natural gas for transportation over long distances come as a consequence of this tendency.
The liquefaction of natural gas requires a high amount of energy that can be recovered during the re-gasification phase. In this paper, a novel approach for this purpose is presented, where the main feature is the use of a combination of Rankine and Brayton cycles while retaining natural gas as the only working fluid of the system.
The proposed system is optimized for cost and exergy efficiency using a bi-level multi-objective optimization procedure, where the master level is setup as a nonlinear optimization problem and solved using an evolutionary algorithm, while the slave level as a mixed integer-linear programming problem. The results of the optimization show that such system can potentially achieve high efficiencies (up to 60 % exergy efficiency for the power cycle and above 65 % plant thermal efficiency), at the cost of a significant capital investment for the heat exchanger network. By allowing a lower level of integration in the system a profitability of up to 98 kUSD/y can be achieved, while retaining significantly high performance.

1. Introduction

Low carbon intensity and high conversion efficiency make natural gas (NG) the best fit for a decarbonizing energy sector. For transporting and storage purposes NG is liquefied by cryogenic refrigeration at about -162 °C into liquefied natural gas (LNG).
As a consequence of the increasing global energy demand and of its potential as a transition fuel, NG production has grown every year since the economic crisis of 2009, reaching 3,613 x 10^9 m^3 of global production in 2016 (IEA, 2017). In this scenario, transporting natural gas in its liquefied form (LNG) will gain increasing relevance over the coming years. The liquefaction of NG is a highly energy-intensive process, but part of the expended energy remains stored in the LNG in the form of cold exergy. At the receiving terminals LNG has to be regasified to be introduced into the gas network and distributed to end users. The vaporization process releases an important amount of cold exergy, of around 370 kJ/kg of LNG (Romero Gómez et al., 2014). While the current practice is to use ambient (sea water, air) or combustion heat as a heat source for LNG regasification, there is significant potential in harvesting the cold exergy stored in the low-temperature LNG (Franco and Casarosa, 2015).
The recovery of the cold exergy stored in LNG was suggested by several authors in the past. A thorough review of such previous efforts can be found in (Kanbur et al., 2017). The direct use of the LNG regasification energy as a low-temperature sink has been widely investigated specially in the industrial sector, in which many processes require heat to be extracted at low temperatures. Examples of this type of application are air separation processes (Mehrpooya et al., 2015), desalination processes (Wang and Chung, 2012), cold storage in the food industry (Messineo and Pann, 2011), and cryogenic CO_2 capture (Zhang et al., 2010). The second main possibility of recovery LNG regasification waste energy, and the one this paper focuses on, relates to its use in power cycles. Romero Gómez et al. (2014) offered a wide review of such systems, which are generally subdivided among direct expansion systems (DES), where the main contribution to the power recovered comes from the expansion of the NG itself, and systems based on the use of one or more secondary fluids (SFS). DES

Please cite this article as: Belfiore F., Baldi F., Marechal F., 2018, Exergy recovery during liquefied natural gas regasification using methane as working fluid , Chemical Engineering Transactions, 70, 535-540 DOI:10.3303/CET1870090

are the simplest and require the lowest installation costs, but also the least efficient (exergy efficiency of around 12 %, Kanbur et al. (2017)). SFS can be based on different principle, such as Brayton cycles (Kaneko et al., 1993), Rankine cycles (Choi et al., 2013), and combined cycles (Stradioto et al., 2015). Another possibility to further improve the efficiency is to combine direct expansion with one or more closed cycles as proposed by Kaneko et al. (2004), who investigated a mirror gas-turbine as a new kind of combined cycle constituted by a conventional gas-turbine as topping cycle and an inverted Brayton cycle as bottoming one.
Most of the high-efficiency plants proposed in literature make use of a combination of several working fluids, thus increasing plant complexity. Among the exceptions, Franco and Casarosa (2015) proposed a multi-stage DES, where the use of two and three pressure levels allowed increasing the efficiency of the system.
This work also focuses on advanced DES, relaying only on NG (considered as pure CH_4) as a working fluid, thus avoiding the complexity of handling additional fluids and reducing the cost of machinery. However, the proposed system also includes the waste heat from a gas engine among the heat sources available to the heat recovery power cycle. The thermodynamic cycle is based on the direct expansion of NG involving a combination of Rankine and Brayton cycles. In addition to the cold exergy supplied the regasification of LNG, heat above ambient temperature is provided by the CHP NG Engine. A system with these features, to the best of the authors' knowledge, has never been suggested in scientific literature before.

2. Methodology

Figure 1 shows the plant scheme. LNG entering the thermodynamic cycle at cryogenic conditions, is pumped at a pressure higher than the one required by the NG distribution line, heated up, expanded to produce electricity and finally delivered to the gas network. Compression and expansion lines are split up in different stages, allowing the integration of a series of closed Rankine and Brayton cycles. In each sub-cycle heat can be supplied either by the NG Engine or by internal heat recovery. The environment can be exploited for heating and cooling needs compatible with the ambient temperature. Electricity can be sold to the grid while the NG not burnt in the engine is delivered to the gas network.
The design is addressed through a bi-level optimization which decomposes the problem in a non-linear (NLP) and a mixed-integer linear (MILP) sub-problems. As shown in Figure 2 each iteration starts with the definition of a new individual by the master level optimizer (step 1). Such step is managed by an in-house developed evolutionary algorithm (Leyland, 2002) capable of solving multi-objective NLP problems. The decision variables hereby defined are then employed by a model of the system developed in flowsheeting software (Belsim VALI) to compute the cycle performance (step 2). During the slave optimization the individual units are sized by solving a MILP problem, based on pinch analysis and implemented in a calculation platform (Bolliger, 2010) using IBM CPLEX® as a solver (step 3). Finally, non-linear plant cost and performance are estimated (step 4) to give a feedback to the evolutionary algorithm which will define a new set of decision variables and start a new iteration. The two optimization stages are explained in more details in the following sections.

2.1 Master optimization

The NLP solved during the master level optimization is represented by Eq(1). Constraints are defined by energy balances and model equations specified in the flowsheeting software environment.

$$\begin{aligned} \min_{x_M} \Big(& \mathrm{C_{inv}}(x_M, y_M), -\eta_{ex,cycle}\,(x_M, y_M)\Big) \\ & s.t.\, g_i(x_M, y_M) \le 0 \\ & \quad h_i(x_M, y_M) = 0 \end{aligned} \tag{1}$$

Problem parameters (y_M) and optimized variables (x_M) are listed in Table 1 and Table 3. To restrict the solution space to feasible solutions, among the decision variables pressure drops and temperature differences were preferred to absolute values when possible.
The annualized investment cost of the power cycle is computed by summing up the cost of all installed machines $C_{inv,i}$ to the one of the heat exchanger network (HEN) C_{HEN}, estimated with the area targeting method, by assuming the minimum number of heat exchangers and a uniform distribution of the total area among them (Kemp, 2007).

$$\mathrm{C}_{inv} = C_{HEN} + \sum_i C_{inv,i} \tag{2}$$

The second objective function, the cycle exergy efficiency $\eta_{ex,cycle}$, is computed through Eq(3) – Eq(4).

$$\eta_{\mathrm{ex,cycle}} = \frac{\dot{P}_{cycle}}{\dot{B}_{CH_4} + \dot{B}_{engine}} \tag{3}$$

$$\dot{\mathrm{B}}_{\mathrm{CH_4}} = \dot{m}_{LNG} \cdot [(\mathrm{h}_{LNG} - \mathrm{h}_0) - T_0 \cdot (s_{LNG} - s_0)] - \dot{m}_{\mathrm{NG}} \cdot [(\mathrm{h}_{NG} - \mathrm{h}_0) - T_0 \cdot (s_{NG} - s_0)] \tag{4}$$

The subscript “0” stands for the ambient conditions (T = 25 °C and p = 1 bar), “LNG” refers to the inlet conditions (T = -161.97 °C and p = 1 bar) and finally “NG” to the outlet ones (T = 25 °C and p = 6 bar). $\dot{B}_{engine}$ represents the exergy content of the heat streams recovered from the engine, listed in Table 2.

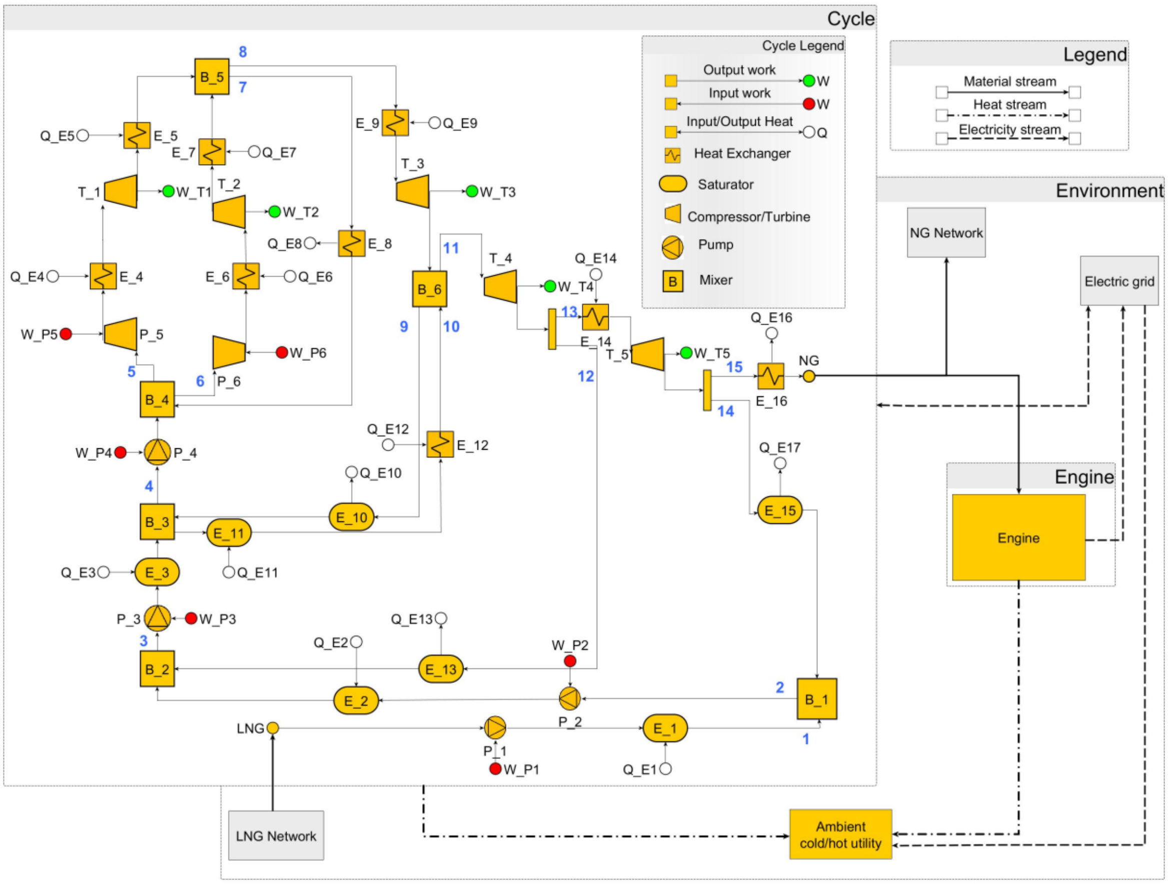

Figure 1: Plant scheme

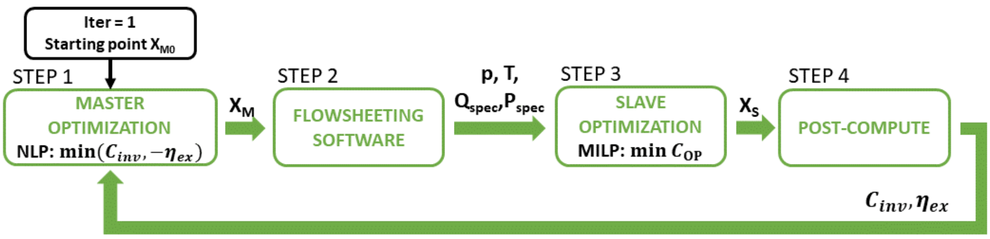

Figure 2: Methodology

2.2 Slave optimization and MILP formulation

The slave optimization aims at sizing the set of machines to be installed by minimizing the annual operating cost, solving the following MILP.

$$\min_{x_S} C_{OP}(x_s, y_s)$$
$$s.t.\, h_i(x_S, y_S) = 0$$
$$g_i(x_S, y_S) \le 0 \tag{5}$$

Problem parameters (y_S) and decision variables (x_S) are listed in Table 1 and Table 3.
A set of potential units ($u \in U$), and their size limitation (f_u^{min} and f_u^{max}) must be defined, as well as the operating period duration (t_{op}). For each unit a binary decision variable (z_u) determines the purchase (i.e. existence) of the unit, while a continuous decision variable (f_u) defines its size. In the current study optimized units are: each single branch of the thermodynamic cycle, the ambient (i.e. cooling/heating capabilities at ambient conditions), the electricity grid and finally the LNG and NG networks.
The operating cost results from the sum of a fixed component $(c_{op,fix})$ associated to the unit usage and a variable one $(c_{op,var})$ related to its operating load (Eq(6)). The only operating costs (revenues) taken into account during the current study are those related to selling the resources (electricity, NG).

$$C_{OP} = \sum_{u \in U} \left[\left(c_{op,fix,u} \cdot z_u + c_{op,var,u} \cdot f_u \right) \cdot t_{op} \right] \tag{6}$$

To guarantee feasibility in heat exchanges (i.e. to satisfy the second principle of thermodynamics) the heat cascade is included among the constraints. Further information about such methodology can be found in (Kemp, 2007).

2.3 Assumptions

Table 1 presents the set of parameters assumed, among which h_x and ΔT_x stand for the heat transfer coefficient and the minimum temperature difference, defined for each thermal stream according to its state: liquid, gaseous, condensing and vaporizing. Resources selling price have been assumed as reported in (Moret, 2017). In Table 2 the heat recovery streams from the NG engine are listed with the respective temperature intervals and thermal efficiency (defined on the NG input basis).

Table 1: List of problem parameters

Parameter	Unit	Value	Parameter	Unit	Value	Parameter	Unit	Value
LNG inlet p	bar	1	Pumps η_{vol}	%	80	h_{gas}	W/m^2/°C	60
LNG inlet T	°C	-161.97	Engine η_{el}	%	44.5	h_{liquid}	W/m^2/°C	560
NG outlet p	bar	6	Electricity selling price	CHF/MWh$_{el}$	90.6	h_{cond}	W/m^2/°C	1,600
NG outlet T	°C	25	NG selling price	CHF/MWh$_{LHV}$	34.82	h_{vap}	W/m^2/°C	3,600
NG outlet m	kg/s	1	Time step duration t_{op}	h/y	8,000	ΔT_{gas}	°C	7
Turbines η_{is}	%	80	Investment life time	y	20	ΔT_{liquid}	°C	5
Compressors η_{is}	%	80	Engine size	kW	2,000	ΔT_{cond}	°C	3
						ΔT_{cond}	°C	2

Table 2: NG engine heat recovery streams

Stream definition	Temperature interval [°C]	Thermal efficiency [%]
Exhaust gas cooler	[400-25]	35.4
Charge air cooler	[90-40]	14.3
Lubricating oil cooler	[80-60]	5.8

3. Results

Figure 3a shows the Pareto frontier obtained with 7,500 evaluations of the evolutionary algorithm. 3.4 s were needed for a complete iteration (i.e. the evaluation of a single individual). Table 3 lists the set of variables defined for the master and slave optimization and their optimized value for the three optimal solutions lying on the Pareto curve and labeled as “Cycle A”, “Cycle B” and “Cycle C” (Figure 3a). Performance and cost of such solutions are reported in Table 4. On the Pareto front, values of the cycle exergy efficiency as high as 60 % are reached and above 65 % for the total plant thermal efficiency, proving the attractiveness of the system investigated. However, under the assumptions made, the economic analysis shows that slightly lower performance must be accepted to guarantee profitable design alternatives (Cycle B). In all the selected solutions, the major portion of the investment is associated to the HEN. To decrease such contribution, designs towards lower investment cost are characterized by a higher exploitation of the ambient to cool down the engine at the expense of the power cycle.

Table 3: Set of optimized variables

Master optimization						Slave optimization					
Variable	Unit	Bounds	Cycle A	Cycle B	Cycle C	Parameter	Unit	Bounds	Cycle A	Cycle B	Cycle C
$P_{P\_3,in}$	bar	[6-20]	13	6.05	6.05	m1	kg/s	[1-2]	1.090	1.090	1.090
$p_{P\_3,out}$	bar	[$p_{P\_3,in}$- 47]	17.36	14.75	14.75	m9	kg/s	[0-2]	0.047	0	0
$p_{P\_5,out}$	bar	[47-100]	75.77	70.17	76.7	m10	kg/s	[0-2]	0	0.005	0.238
$p_{P\_6,out}$	bar	[100-300]	248.2	244.3	203.3	m6	kg/s	[0-2]	1.672	1.244	0.981
ΔT_{E_4}	°C	[200-500]	236.63	273.2	274.6	m7	kg/s	[0-2]	0.199	0	0
ΔT_{E_5}	°C	[-200-200]	101.34	75.9	76.9	m12	kg/s	[0-2]	0.169	0.159	0.148
ΔT_{E_6}	°C	[200-500]	423.67	447.8	235	m14	kg/s	[0-2]	0.167	0	0
ΔT_{E_9}	°C	[0-100]	0	37.4	0	Amb. cooling	MWth	[0-2]	0.57	0.68	1.02
ΔT_{E_13}	°C	[-20-100]	-7.43	-4.9	10.3	Amb. heating	MWth	[0-2]	0	0	0
B_4 split	-	[0-1]	0	0	0.02	Elect. sold	MWel	[0-10]	2.933	2.827	2.488

Table 4: Plant and cycle cost and performance

Variable	Unit	Cycle A	Cycle B	Cycle C
Total annualized cost	kUSD/y	250.5	-98	-15
Total annualized Investment cost	kUSD/y	1,175	745	568
HEN annualized investment cost	kUSD/y	1,008	599	451
Operating cost	kUSD/y	-925	-843	-583
Cycle power	kW	937.2	832	494.7
Exergy efficiency	%	60.38	53.62	31.88
Cycle thermal efficiency	%	35.61	37.09	28.16
Plant thermal efficiency	%	65.35	63.02	55.5
HEN area	m^2	1548	939.6	247

(a) (b)

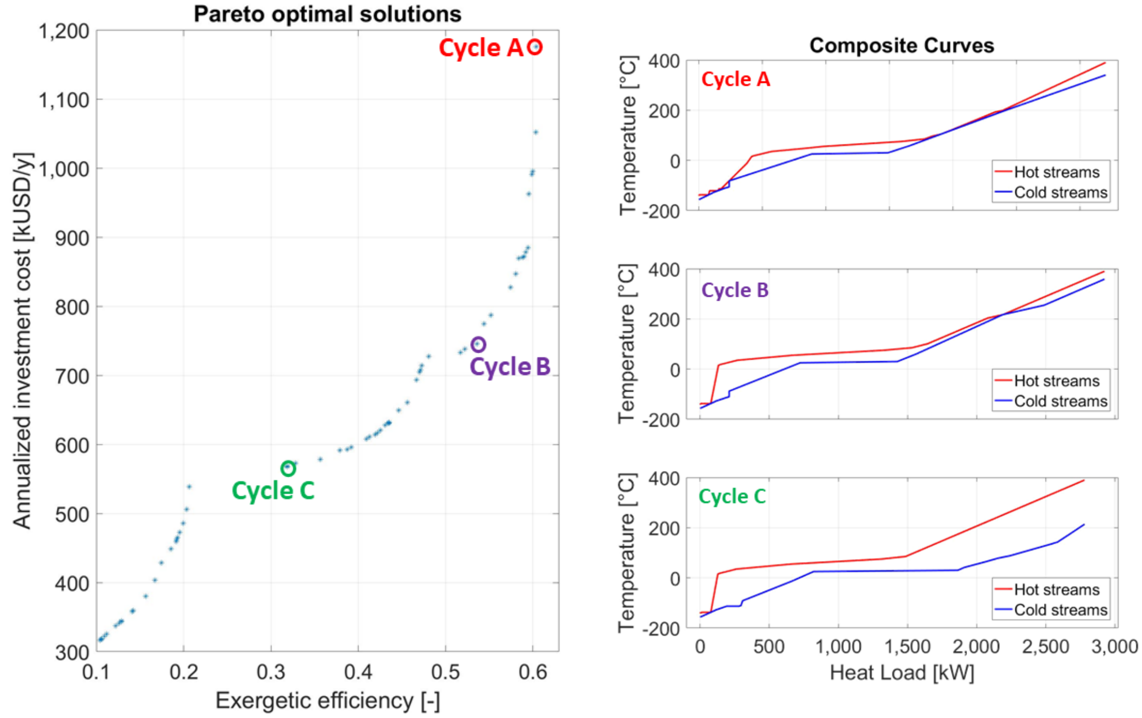

Figure 3: Pareto frontier (a) and Composite Curves (b)

However, it must be noted that there is a high uncertainty in the estimation of the HEN investment cost due to the use of the area targeting method. In addition, the heat exchangers dealing with fluid in supercritical conditions were subdivided in several “virtual” stages to improve the fidelity of the modelling, thus leading to an overestimation of the number of heat exchangers required and, hence, of the related investment cost. The use of more advanced methods for HEN cost estimation and optimization, such as the one proposed by (Mian et al., 2016), could provide more accurate results. Results show that none of the solutions on the Pareto frontier takes advantage of the lower pressure level in the supercritical region and configurations towards lower investment costs do not integrate the gas cycle. Finally, from the analysis of the composite curves (in Figure 3b corrected according to the ΔT_x listed in Table 1), the authors believe that the cycle performance could be further improved by enhancing the superstructure adopted, hence allowing a higher degree of integration.

4. Conclusions

In the current study an innovative power cycle for the cold exergy recovery during the LNG regasification was investigated. The power cycle is based on the integration of multi-stage Rankine and Brayton cycles with a CHP NG engine. A superstructure of different pressure levels was introduced to grant flexibility to the model, while process integration techniques were exploited to explore different design alternatives. A bi-level optimization coupling a multi-objective NLP and a MILP sub-problem was adopted to define the thermodynamics of the power cycle and the machines size. Results have shown cycle exergetic efficiency up to 60 % and plant thermal efficiency above 65 %. The optimization suggests that profits as high as 98 kUSD/y can be achieved while retaining significantly high performance.

References

Belsim VALI, 2018, <www.belsim.com/vali>, accessed 20/04/2018.

Bolliger R., 2010, Methodology of the synthesis of industrial energy systems, PhD Thesis, École Polytechnique Fédérale de Lausanne, Lausanne, Switzerland. (in French)

Choi I.H., Lee S., Seo Y., Chang D., 2013, Analysis and optimization of cascade Rankine cycle for liquefied natural gas cold energy recovery, Energy, 61, 179–195.

Franco A., Casarosa C., 2015, Thermodynamic analysis of direct expansion configurations for electricity production by LNG cold energy recovery, Applied Thermal Engineering, 78, 649–657.

International Energy Agency (IEA), 2017, Natural gas information, <www.iea.org/publications/freepublications/publication/NaturalGasInformation2017Overview.pdf>, accessed 20/04/2018.

Kanbur B.B., Xiang L., Dubey S., Choo F.H., Duan F., 2017, Cold utilization systems of LNG: A review, Renewable and Sustainable Energy Reviews, 79, 1171-1188.

Kaneko K., Ohtani K., Tsujikawa Y., Fujii S., 2004, Utilization of the cryogenic exergy of LNG by a mirror gas-turbine, Applied Energy, 79, 355–369.

Kemp I.C., 2007, Pinch Analysis and Process Integration, Elsevier, Oxford, United Kingdom.

Leyland G.B., 2002, Multi-objective optimization applied to industrial energy problems, PhD Thesis, École Polytechnique Fédérale de Lausanne, Lausanne, Switzerland.

Mehrpooya M., Sharifzadeh M.M.M., Rosen M.A., 2015, Optimum design and exergy analysis of a novel cryogenic air separation process with LNG (liquefied natural gas) cold energy utilization, Energy, 90, 2047–2069.

Messineo A., Pann G., 2011, LNG cold energy use in agro-food industry: a case study in Sicily. Journal of Natural Gas Science and Engineering, 3, 356–363.

Mian A., Martelli E., Maréchal F., 2016, Framework for the multiperiod sequential synthesis of heat exchanger networks with selection, design, and scheduling of multiple utilities, Industrial & Engineering Chemestry Research, 55, 168-186.

Moret S., 2017, Strategic energy planning under uncertainty, PhD thesis, École Polytechnique Fédérale de Lausanne, Lausanne, Switzerland.

Romero Gómez M., Ferreiro Garcia R., Romero Gómez J., Carbia Carril J., 2014, Review of thermal cycles exploiting the exergy of liquefied natural gas in the regasification process, Renewable and Sustainable Energy Reviews, 38, 781-795.

Stradioto D.A., Seelig M.F., Schneider P.S., 2015, Performance analysis of a CCGT power plant integrated to a LNG regasification process, Journal of Natural Gas Science and Engineering, 23, 112–117.

Wang P., Chung T.S., 2012, A conceptual demonstration of freeze desalination-membrane distillation (FD-MD) hybrid desalination process utilizing liquefied natural gas (LNG) cold energy, Water Resources, 46, 4037–4052.

Zhang N., Lior N., Liu M., Han W., 2010, COOLCEP (cool clean efficient power): a novel CO_2 capturing oxy-fuel power system with LNG (liquefied natural gas) coldness energy utilization, Energy, 35, 1200–1210.